

# Rotogravure Printing of Li Ion Battery Anodes

Kevin Matthew, Alexandra Pekarovicova, and Paul Dan Fleming III

Keywords: conductive ink, formulation, rotogravure, anodes, batteries

## Abstract

Rotogravure inks were formulated for Li-ion battery anodes. Different polymer chemistries were tested such as polyvinylidene fluoride (PVDF) with degree of polymerization of  $10^6 - 500,000$ . It was found that best printability can be achieved using mixed PVDF-PVP (polyvinylidene fluoride - polyvinylpyrrolidone) binders with commercial names of PVDF being Kureha 9100, 9300, and Solef 5300. As active materials, Philips 5, 10, 15 graphites (5 -15 micron) in combination with nanocarbon filler were used. Inks were dispersed in NMP (N-methyl-pyrrolidone) solvent. Particle size of graphite for most uniform printing was found to be 5 microns. Surface energy of copper foil substrate and surface tension of inks were determined. Printed copper foils were assembled into battery half cells and their irreversible capacity loss (ICL) was tested. The ICL was lower when mixed PVDF/PVP binder was employed in anode ink.

## Introduction

The latest printing technologies implemented in printed electronic devices (including electrochemical devices) can be broadly divided into the master image carrier and non-master image carrier methods. The master image carrier printing process can be further divided into screen printing, rotogravure printing, and flexographic printing. Printing technologies without master image carrier mainly include inkjet and 3D printing. These printing methods rely on the local and controlled distribution of ink onto the receiving material in a template-less manner (Kim, 2017).

The use of printing processes in battery manufacturing can lead to mass production of flexible batteries (Arduini, 2016). Printing can produce flexible batteries with different design patterns, and their multilayer printing stack can shape the geometry and structure of the battery and improve its electrochemical performance. There are usually two types of the printed structures of printed batteries, such as stack or sandwich architecture and the coplanar or parallel architecture. Components used

---

Western Michigan University

for anode, anode, separator, electrolyte, cathode, and current collectors deposited on the flexible substrate are shown in the Figure 1 (Lanceros, 2018).

Printing inks for anode and cathode inks include active materials such as graphite, or active fillers – nanocarbons, and resins or binders which were selected based on ink chemistry whether ink was solvent, or water based. Resins can include lithiated polyacrylic acid, or polyvinylidene fluoride of different degree of polymerization. Printed layers should be thick, preferably up to 100micron and therefore screenprinting is the process of choice. In this work, the aim was to formulate rotogravure printing inks and evaluate their printability in terms of print uniformity, thickness of the layers and ultimately, battery performance.

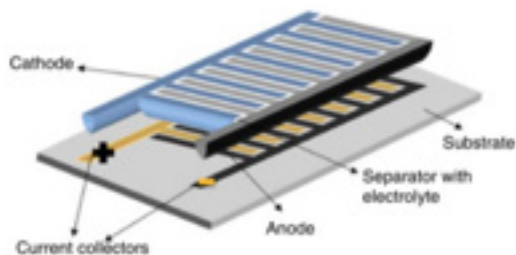


*Figure 1: Example of the stack or sandwich battery architecture (Lanceros, 2018)*

### **Experimental Procedure**

Timcal C45 device was used for mixing the inks. As the conductive graphite Philips 5 $\mu$ m, 10 $\mu$ m, 15 $\mu$ m and Mage 3 graphite were used. Kureha 9100 polymer (PVDF) with a molecular weight of 2.8x10<sup>5</sup> was dissolved in N-methyl-2-pyrrolidone (NMP) solvent and used as the vehicle. In some inks, polyvinylidene/polyvinylpyrrolidone mix of binders (PVDF-PVP) was employed. Printing was done on Cu foil.

Rotogravure plate for RK gravure K-proofer was engraved in WRE/ColorTech with proprietary engraving at 75 LPI. New plate was engraved with 1000, 500, 250 and 100  $\mu$ m hole shaped nonimage areas. Detail of 500  $\mu$ m nonimage area is shown in the Figure 2 and white light interferometry detail is shown at Figure 3, showing depth of cells at 75  $\mu$ m and cell opening in one direction at 1194  $\mu$ m. Engraving was done by hybrid process of laser ablation and chemical etching.

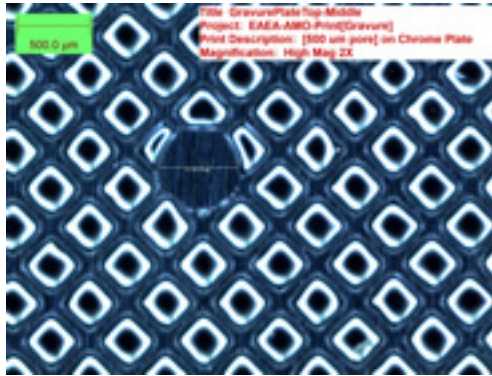


*Figure 2: Detail of new gravure engraved plate (by WRE Color/Tech) with 500 µm nonimage area (hole)*

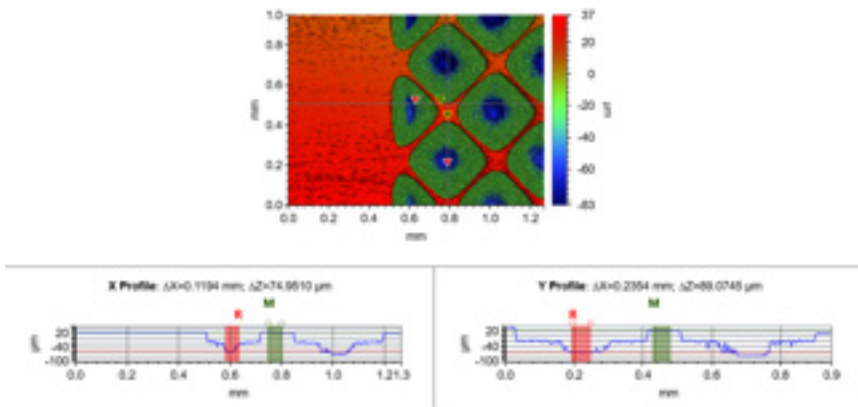


*Figure 3: White light interferometry of gravure engraved plate*

Profile of the plate and ink films was done on Bruker white light interferometry instrument. Image analysis of printed ink films was done using Pax it 2 software.

## Results and Discussion

Some of the inks prepared for rotogravure printing on copper foil along with their performance are listed in the Table 1.

Ink formulation (Graphite/Carbon black/Binder)	Particle size (Graphite/CB)	Ratio (Graphite/CB /Binder)	Solid content (SC) [%]	Print quality
Philips 15um/ C45/Kureha 9100	15um/37nm	92/2/6	30, 40, 50	Poor
Philips 10um/ C45/Kureha 9100	10um/37nm	92/2/6	30, 40, 50	Better, but still insufficient
1 Philips 5um/ C45/Kureha 9100	5um/37nm	92/2/6	30, 40, 50	Non-uniform
Philips 5um/C45/ Kureha 9300	5um/37nm	92/2/6	30, 40, 50	Non-uniform
2 Philips 5um/ C45/Kureha 9100	5um/37nm	80/5/15	30, 40, 50	Better, but visible holes
Argonne G/C45/ Kureha 9300	5um (spherical) /37nm	80/5/15	30, 40, 50	Non-uniform
Nanoramic G/ C45/Kureha 9300	3-5um/37nm	80/5/15	30, 40, 50	Non-uniform
Silicon/C45/PAA (Li <sup>+</sup> )	150nm/37nm	70/10/20	30, 40, 50	Uniform smooth print

**Table 1:** Ink formulations used for gravure printing (C45- nanocarbon active filler)

When we started to print, it was not clear what resolution of gravure plate to use. 120-75 LPI (lines per inch) resolution of engraving was tested. Since lower resolution (LPI count) plates consist of larger gravure cells, the plate was lowered to a 100 LPI plate and Philips 5µm graphite at 50%, 45%, 40% and 30% solid content inks were printed to study its effect on the printability. The initial prints were poor, so resolution was decreased to 75 LPI and same solid contents were tested.

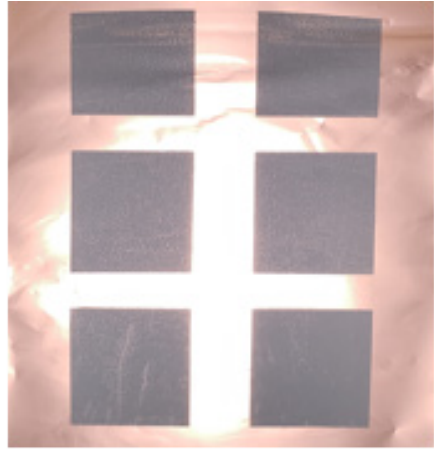
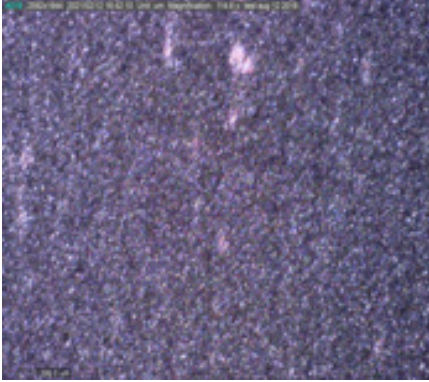


**Figure 4:** (left) Magnified surface image (right) Philips 5µm at 40% SC 75 LPI.

Figure 4 shows relatively uniform print using Philips 5µm graphite. In order to improve print uniformity and ink coverage, inks of the ratio 80/5/15 graphite/conductive nanoparticle carbon/binder were prepared using C45 conductive nanoparticle carbon and Kureha 9300 binder. Also, new graphites used were 3-5µm graphite from Nanoramic (Figure 5) and 5µm spherical graphite from Argonne National Laboratory (Figure 6), respectively. Prints were made for 25%, 30% and 35% solid contents. An ink consisting of 150nm particle size silicon at 10-15% solid content was also formulated and tried to confirm effect of particle size on its printability for gravure (Figure 7).

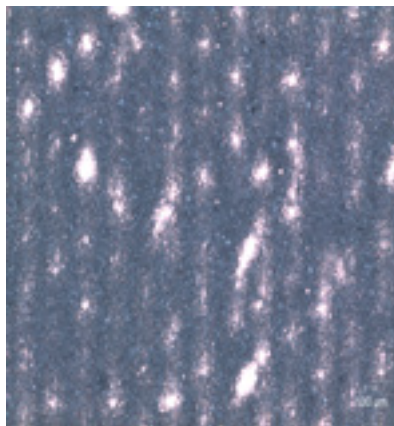


**Figure 5:** Magnified surface image of Nanoramic graphite at 30% SC

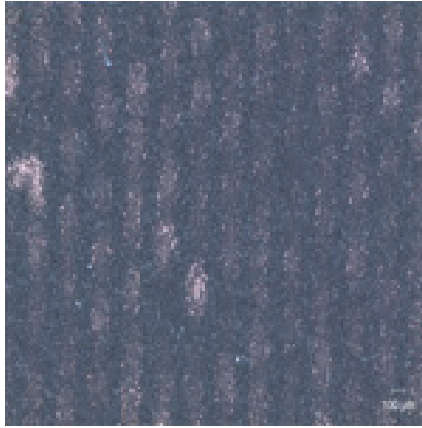


**Figure 6:** Magnified surface images of Argonne spherical graphite at 30% SC

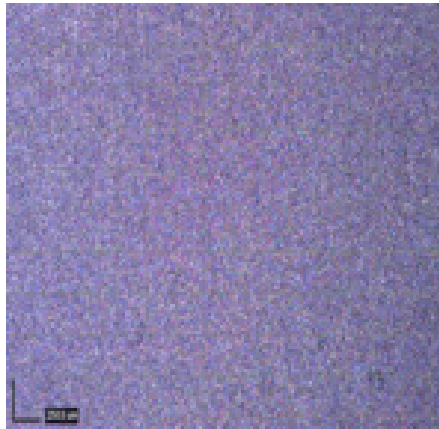


**Figure 7:** Magnified surface images of Silicon ink at 13% SC

Slight improvements can be observed with changes to particle size and morphologies of the graphite, using Nanoramic graphite (Figure 5) or Argonne spherical graphite (Figure 6), but the print non-uniformity still posed problems. However, when the particle size was reduced to 150nm in the case of the silicon ink using a polyacrylic binder (Li-PAA) in the ratio of 70/10/20, at 13% solid content, a smooth and uniform print could finally be observed (Figure 7).

Inks with N-methyl pyrrolidone (NMP) as a solvent with long chain (PVDF) polymers such as Kureha 9300 or Solef 5130 did not result in successful ink coverage. Ink most likely cannot enter and exit gravure cells. It is clearly visible in Figure 8, where print was done using spheric graphite/ nanocarbon C45 and Solef 5130 resin at 33% solids.

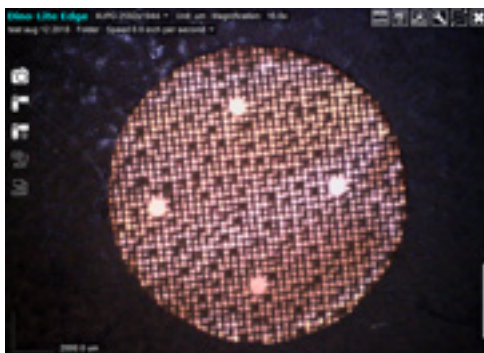


**Figure 8 :** Detail of print on 75 LPI plate with 500 µm nonimage area SG/C45/5130- 90/3/7 at 33% SC

A new resin, polyvinylpyrrolidone at 10,000 molecular weight was used to disperse graphite and nanocarbon active material. Inks with 30 - 72% solids were made. Inks were formulated with Philips graphite with 5 micron particle size, P5/CB 4400/ PVP (80:5:15). As a solvent, ethanol or NMP were used. Ethanol was evaporating too fast, thus NMP was chosen (Figure 9). Average surface tension of NMP ink with 70% solids was 39.4 mN/m and its average contact angle with copper surface was 40.8 deg.

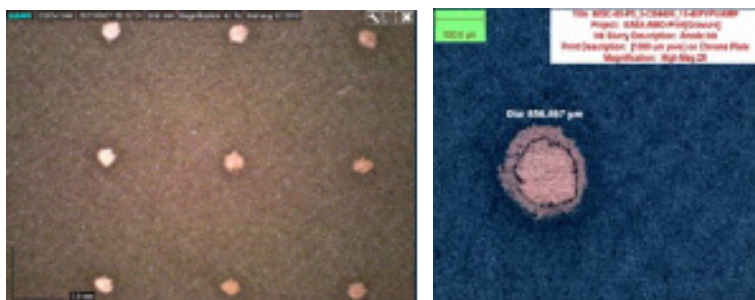


**Figure 9:** Detail of NMP ink with PVP resin showing print with 1000 µm non image areas

Gravure prints with NMP as a solvent were easier to work with than using inks with water or ethanol as a solvent. Inks were finally printing uniformly. Designed holes with diameter 1000 µm were printing as  $846 \pm 20$  µm diameter, while 500 µm holes were printed as  $219 \pm 11$  µm (Figure 10). At 70% solids, ink layers were 25 - 27 µm thick with mass loading of 2.1 - 2.5 mg/cm<sup>2</sup>. Half cells were made as control and print with 1000 µm holes. Performance of PVP half cell batteries was not sufficient (data not shown). PVP was then mixed with PVDF – Kureha 9100 or Kureha 9300 and half cells were made again. Their performance in terms of irreversible capacity loss (ICL) was tested (Fig. 11). Inks were bar coated not gravure printed to ensure higher thickness of layers then possible with gravure printing.

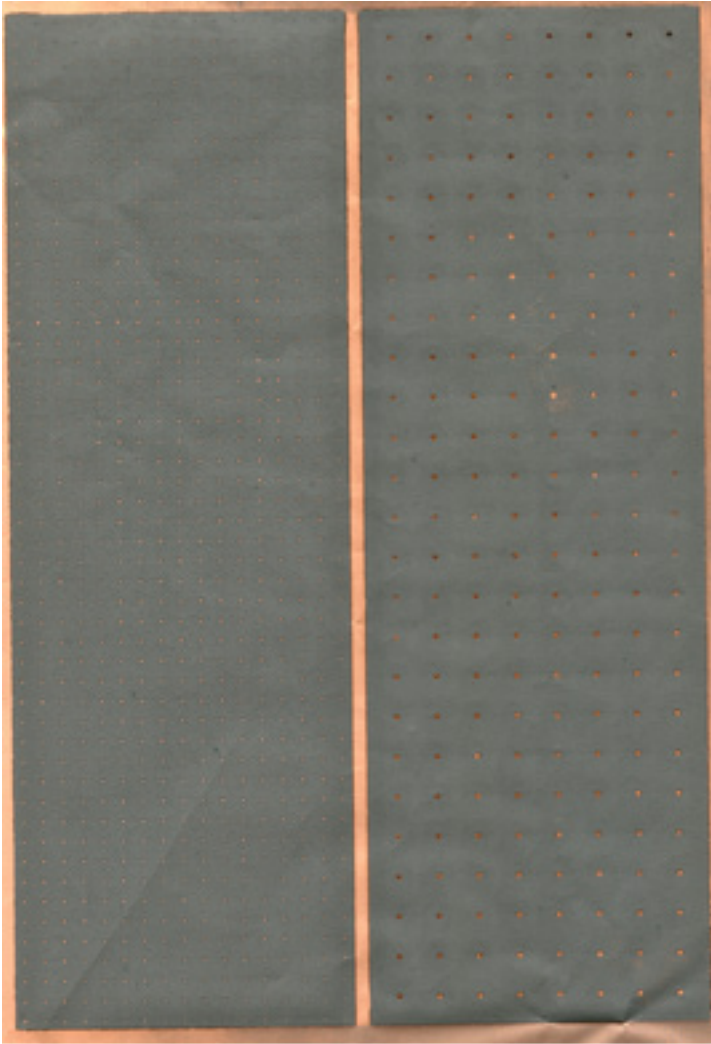


*Figure 10: P5/4400/PVP- 80/5/15 (PVP in NMP at 70% solids) 500  $\mu\text{m}$  and 1000  $\mu\text{m}$  pores*



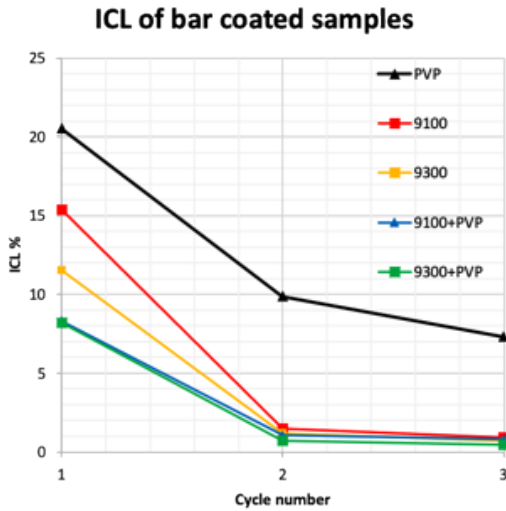


**Figure 11:** Comparison of battery performance (as irreversible capacity loss, ICL) of sole PVP, sole PVDF or combination PVP/PVDF

From the Fig. 11 can be seen that performance of mixed PVP/PVDF inks was greatly improved, and mixed PVP/PVDF achieve actually slightly better performance and suffer from smaller ICL, than inks made with sole Kureha 9100 or 9300.

### Conclusions

Among P5-15 graphites, P5 graphite has optimum printability and battery performance. Increasing particle size of graphite did not improve print quality of PVP inks. PVP showed good printability but poor battery performance. Using mixed PVP/PVDF 9300 or PVP/PVDF 9100 binder combination could effectively improve battery performance without significantly sacrificing the printability.

### Acknowledgement

This work was funded through DOE Advanced Manufacturing Office (DE-EE0009111) Wu Q. et al: Enabling Advanced Electrode Architecture through Printing and Pekarovicova A. : GEF-PGSF Gravure Day, 2021 grant.

## References

Arduini, F., V. Scognamiglio, D. Moscone, G. Palleschi, in: *Biosensors for Security and Bioterrorism Applications*, Springer, Switzerland (2016). [https://link-springer-com.libproxy.library.wmich.edu/chapter/10.1007%2F978-3-319-28926-7\\_6](https://link-springer-com.libproxy.library.wmich.edu/chapter/10.1007%2F978-3-319-28926-7_6)

Kim, J., Kumar, R., Bandodkar, A. J., Wang, J., *Advanced Materials for Printed Wearable Electrochemical Devices: A Review*. *Adv. Electron. Mater.* 2017, 3, 1600260. <https://onlinelibrary-wiley-com.libproxy.library.wmich.edu/doi/full/10.1002/aelm.201600260#aelm201600260-bib-0098>

Lanceros-Méndez, S., Costa C. M., John Wiley & Sons, *Printed Batteries: Materials, Technologies and Applications*, Feb 23, 2018. [https://books.google.com/books?hl=en&lr=&id=WnFODwAAQBAJ&oi=fnd&pg=PA1&dq=anode+inks+for+batteries+printed+by+flexo&ots=UhPyJg5FVa&sig=fPthiMLIdcd2qTuwPx-sgO0cB\\_uc#v=onepage&q=anode%20inks%20for%20batteries%20printed%20by%20flexo&f=false](https://books.google.com/books?hl=en&lr=&id=WnFODwAAQBAJ&oi=fnd&pg=PA1&dq=anode+inks+for+batteries+printed+by+flexo&ots=UhPyJg5FVa&sig=fPthiMLIdcd2qTuwPx-sgO0cB_uc#v=onepage&q=anode%20inks%20for%20batteries%20printed%20by%20flexo&f=false)